



# Effect of oxygen content on CO<sub>2</sub> absorption characteristics of Li<sub>2</sub>TiO<sub>3</sub>

Furuyama, Yuichi ; Nakamura, Hodaka ; Takeda, Tsubasa ; Samata, Hiroaki ; Taniike, Akira ; Kitamura, Akira

---

## (Citation)

Nuclear Materials and Energy, 15:164-168

## (Issue Date)

2018-05

## (Resource Type)

journal article

## (Version)

Version of Record

## (Rights)

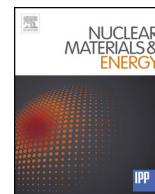
© 2018 Elsevier Ltd.

This is an open access article under the CC BY-NC-ND license (<http://creativecommons.org/licenses/by-nc-nd/4.0/>).

## (URL)

<https://hdl.handle.net/20.500.14094/90005262>





# Effect of oxygen content on CO<sub>2</sub> absorption characteristics of Li<sub>2</sub>TiO<sub>3</sub>

Yuichi Furuyama\*, Hodaka Nakamura, Tsubasa Takeda, Hiroaki Samata, Akira Taniike, Akira Kitamura

Graduate School of Maritime Sciences, Kobe University, Kobe 658-0022, Japan

## ARTICLE INFO

### Keywords:

Li<sub>2</sub>TiO<sub>3</sub>  
XRD  
NRBS  
ERD  
CO<sub>2</sub> absorption  
Water vapor catalysis

## ABSTRACT

In order to investigate the CO<sub>2</sub> absorption characteristics of the low- and high-density Li<sub>2</sub>TiO<sub>3</sub> samples, X-ray diffraction (XRD), non-Rutherford backscattering spectroscopy (NRBS) and elastic recoil detection (ERD) analyses have been performed. Crystallographic structure of a sintered and CO<sub>2</sub> exposed samples is decided by the XRD analysis, and the NRBS and ERD analyses have evaluated the amount of CO<sub>2</sub> absorption and H content quantitatively. The CO<sub>2</sub> absorption characteristics of the non-stoichiometric Li<sub>2</sub>TiO<sub>3</sub> sample are investigated. It is found that the CO<sub>2</sub> absorption rate of the non-stoichiometric Li<sub>2</sub>TiO<sub>3</sub> sample is much larger than that of the stoichiometric sample. The Li<sub>2</sub>TiO<sub>3</sub> sample (80%T.D.) has a good tritium release characteristics, and we find also that the sample sintered at temperatures higher than 1,428 K absorb very little CO<sub>2</sub> under high humidity conditions. The amount of CO<sub>2</sub> absorption of the low-density Li<sub>2</sub>TiO<sub>3</sub> samples is found to increase with increase in the humidity. This seems to be a catalytic effect of water vapor on CO<sub>2</sub> absorption at the Li<sub>2</sub>TiO<sub>3</sub> surface.

## 1. Introduction

Li<sub>2</sub>TiO<sub>3</sub> has excellent chemical properties such as non-reactivity with H<sub>2</sub>O and relatively good T breeding properties among the solid blanket materials [1–9]. However, our research showed that Li<sub>2</sub>TiO<sub>3</sub> material absorbed CO<sub>2</sub> at room temperature [10–12]. The C contamination of a blanket material should be minimized. It has been reported that C atoms included in a blanket material can form a tritiated hydrocarbon in a T recovery process [13,14]. Therefore, if a blanket material has C contamination, the T recovery efficiency would be decreased, because additional process of isotope separation would be required. However, the CO<sub>2</sub> absorption characteristics of Li<sub>2</sub>TiO<sub>3</sub> have not been fully studied yet [15].

We have been investigating the CO<sub>2</sub> absorption characteristics of Li<sub>2</sub>TiO<sub>3</sub>, and showed that CO<sub>2</sub> absorption of the low-density sample (39%T.D. – 41%T.D.) at room temperature was observed at the dry CO<sub>2</sub> gas, the atmospheric, the dry air and the moist air exposures. On the other hand, the CO<sub>2</sub> absorption of the high-density sample (91%T.D.) was not appreciable. The low-density Li<sub>2</sub>TiO<sub>3</sub> sample has more defects such as vacancies and micro-pores in the crystal grains of the sample compared with the high-density sample.

In the present work, we investigate the CO<sub>2</sub> absorption characteristics of a non-stoichiometric Li<sub>2</sub>TiO<sub>3</sub> sample with defects of O and Li deficiencies caused by re-sintering the sample under an Ar gas atmosphere using an electric tube furnace. The sample is exposed to the dry

CO<sub>2</sub> gas and the amount of CO<sub>2</sub> absorption with respect to the exposure time is investigated.

A suitable density of Li<sub>2</sub>TiO<sub>3</sub> sample for a good T release property is about 80% T.D. [16–19]. We investigate materials which have good T release characteristics and do not absorb CO<sub>2</sub>.

We have investigated the dependence of CO<sub>2</sub> absorption in the low-density Li<sub>2</sub>TiO<sub>3</sub> sample on exposure time to the atmosphere, the dry air and the moist air. In this work, we measure the amount of H content and absorbed amount of CO<sub>2</sub> in the sample with ERD and NRBS analyses, and investigate the influence of the humidity in the exposure environment on CO<sub>2</sub> absorption.

In order to investigate the CO<sub>2</sub> absorption properties, X-ray diffraction (XRD) in addition to the non-Rutherford backscattering spectroscopy (NRBS) and the elastic recoil detection (ERD) analyses mentioned above are carried out to the samples before and after the exposures, and crystallographic structure of the exposed samples and the amount of CO<sub>2</sub> absorption and H content in the Li<sub>2</sub>TiO<sub>3</sub> sample are investigated.

## 2. Experimental

The Li<sub>2</sub>TiO<sub>3</sub> sample used in the present work was prepared by a solid phase reaction method with Li<sub>2</sub>CO<sub>3</sub> and TiO<sub>2</sub> powders. The molded sample was sintered at temperatures from 973 K to 1,500 K using an electric furnace. The sintering conditions for the samples are

\* Corresponding author.

E-mail address: [furuyama@maritime.kobe-u.ac.jp](mailto:furuyama@maritime.kobe-u.ac.jp) (Y. Furuyama).

**Table 1**  
Sintering parameters and heat treatment conditions of the  $\text{Li}_2\text{TiO}_3$  samples.

Li <sub>2</sub> CO <sub>3</sub> : TiO <sub>2</sub> (molar ratio)	Pre-sintering condition		Press condition	Main sintering condition		Sample density [%T.D.]	
	Temperature [K]	Time [h]		Temperature [K]	Time [h]		
1.0 : 1.0			40 MPa 3min	1,000	5	39	
						40	
						41	
	1,000	5		1,173	8	76	
				1,250		85	
	973			1,473	40	91	
	94						
	1,000			Heat treatment conditions	1st:1,500	8	80
					2nd:1,000	10	
		10			873(Ar gas)	24	39

summarized in Table 1. The low-density  $\text{Li}_2\text{TiO}_3$  samples were made by sintering for 5 h at temperatures of 1,000 K. As theoretical mass density of  $\text{Li}_2\text{TiO}_3$  is  $3.43 \text{ g/cm}^3$ , the ratio of the sample mass density to the theoretical mass density was 0.40, which we call “40%T.D.”.

The high-density sample was made by re-sintering the presintered low-density samples as the starting materials. After pulverizing the presintered samples again and molding them, we sintered the samples at 1,473 K for 40 h to get high density up to 94%T.D. To prepare a non-stoichiometric  $\text{Li}_2\text{TiO}_3$  sample, the low-density  $\text{Li}_2\text{TiO}_3$  sample (39% T.D.) was re-sintered in Ar gas atmosphere at 873 K for 24 h using an electric tubular furnace. The sintered samples were disk-shaped with thickness of 2 mm and diameter of 15 mm. We measured the sample mass with a microbalance and the volume with a vernier caliper to calculate the density.

The samples were put in a vacuum chamber evacuated to a pressure of 1 Pa, and were exposed at room temperature to the dry  $\text{CO}_2$  gas, the atmosphere or the moist air at 1 atm. In the case of exposure to the moist air, we set a beaker filled with water in the chamber kept at high humidity ( $>34,000$  ppm). A digital thermo-hygrometer FL-02 was set in the vacuum chamber. The humidity during exposure to the dry  $\text{CO}_2$  gas and the dry air was less than 5,000 ppm, while that during exposure to the atmosphere was 20,000–30,000 ppm.

Samples used in this work were Li compounds,  $\text{Li}_2\text{TiO}_3$ . The NRBS analysis is highly sensitive to Li isotopes, and is very effective for blanket material analysis [20]. The ERD analysis is suitable for measuring H distribution from sample surface region. Placing the sample at the center of the target vacuum chamber, the NRBS analysis was performed using 2.6-MeV-proton beams and a silicon surface barrier detector (SSBD) located at  $165^\circ$  while for ERD analysis 3.0-MeV- $\text{He}^{2+}$  beams and SSBD located at  $30^\circ$  with respect to the direction of the beam incidence. The energy resolution (FWHM) of the NRBS measurement system is 30 keV for C(p,p) and 80 keV for Ti(p,p), which corresponds to the depth resolution of 100 nm and 150 nm, respectively, while the ERD resolution is 80 keV for H(He,p) corresponding to 140 nm.

The crystallographic structure of the prepared  $\text{Li}_2\text{TiO}_3$  samples was

investigated by XRD analysis using RINT2000 (Rigaku) with Cu-K $\alpha$  X-ray at room temperature. The simulation of powder XRD patterns was performed using a Rietveld-analysis program RIETAN and the crystal data for  $\text{Li}_2\text{TiO}_3$ ,  $\text{Li}_2\text{CO}_3$ , and  $\text{TiO}_2$ .

### 3. Results and discussion

#### 3.1. $\text{CO}_2$ absorption characteristics in the non-stoichiometric composition of a $\text{Li}_2\text{TiO}_3$ sample with defects of O and Li deficiencies

Our previous studies have shown that high-density  $\text{Li}_2\text{TiO}_3$  samples with 90% to 95% T. D. hardly absorb  $\text{CO}_2$ . In order to prepare reference data on  $\text{CO}_2$  absorption characteristics,  $\text{Li}_2\text{TiO}_3$  samples with low-density (39–41% T.D.) were mainly used in this section. The dry  $\text{CO}_2$  gas exposure of the low-density  $\text{Li}_2\text{TiO}_3$  sample (39%T.D.) was performed in the dry  $\text{CO}_2$  gas-filled vacuum chamber at 1 atm at room temperature. The exposure time was 2,000 h at the maximum.

XRD analysis was performed on the low-density  $\text{Li}_2\text{TiO}_3$  samples (39%T.D.) after exposure to the dry  $\text{CO}_2$  gas in order to investigate crystallographic structure change of  $\text{Li}_2\text{TiO}_3$ . Fig. 1 shows the powder XRD spectra in comparison with the typical as-sintered  $\text{Li}_2\text{TiO}_3$  sample (39%T.D.), where X-ray intensity is recorded as a function of the diffraction angle  $2\theta$ . Simulation spectra of  $\text{Li}_2\text{TiO}_3$ ,  $\text{Li}_2\text{CO}_3$  and  $\text{TiO}_2$  are also shown in this figure.

The powder XRD spectral pattern of the as-sintered sample is in good agreement with the simulation spectrum; peaks are observed at  $2\theta = 19^\circ, 36^\circ, 44^\circ, 48^\circ, 58^\circ, 63^\circ$  and  $67^\circ$ , which indicates that the sintered samples are converted almost perfectly to  $\text{Li}_2\text{TiO}_3$ . In the spectrum of the low-density  $\text{Li}_2\text{TiO}_3$  sample after the exposure to the dry  $\text{CO}_2$  gas for 2,000 h, the XRD peaks of  $\text{Li}_2\text{CO}_3$  are observed at  $2\theta = 21^\circ, 31^\circ$ , and  $32^\circ$ . This clearly indicates that  $\text{Li}_2\text{TiO}_3$  absorbs  $\text{CO}_2$  and then forms  $\text{Li}_2\text{CO}_3$  and  $\text{TiO}_2$  by the dry  $\text{CO}_2$  gas exposure.

A non-stoichiometric composition  $\text{Li}_2\text{TiO}_3$  sample (39%T.D.) was prepared in an Ar gas atmosphere using an electric tube furnace. The NRBS spectra of the non-stoichiometric composition  $\text{Li}_2\text{TiO}_3$  sample

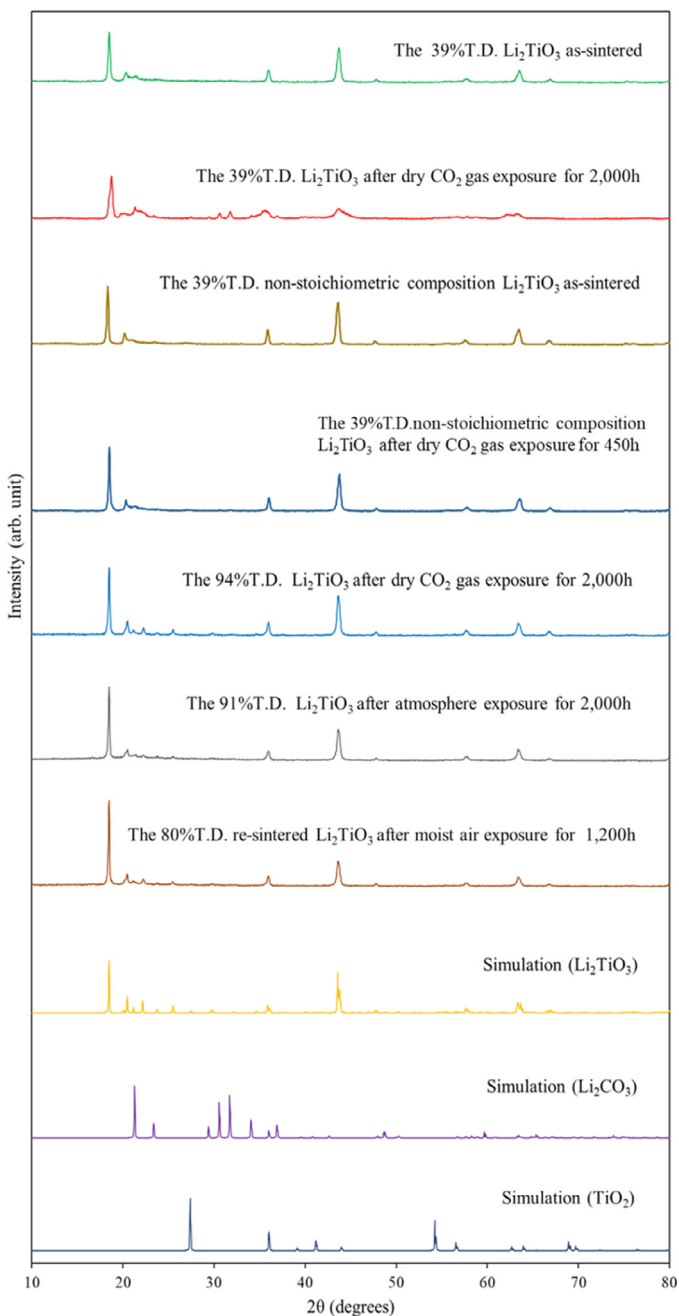


**Fig. 1.** XRD patterns of the as-sintered low-density and high-density  $\text{Li}_2\text{TiO}_3$  samples and changes of XRD patterns after exposures to the dry  $\text{CO}_2$  gas, the atmosphere and the moist air.

(39%T.D.) before and after the dry  $\text{CO}_2$  gas exposure for 800 h was shown in Fig. 2a. In this figure, the scattered particle yield is plotted as a function of energy. For comparison, the NRBS spectrum of this sample before exposure (as-sintered sample) is also shown. The edge energies of Ti, O, C, and Li spectra are about 2.4, 2.0, 1.8, and 1.5 MeV, respectively. A C(p,p) proton spectral peak, which was absent before the dry  $\text{CO}_2$  gas exposure, appeared, and the O(p,p) yield increased after the dry  $\text{CO}_2$  gas exposure.

Fig. 2b shows depth distribution of Li, C, O and Ti deduced from the energy spectra. The reason for the apparent non-zero densities in the negative depth region and the finite width of the up edges at the surface is a finite energy resolution of the detection system. The spectra are not corrected for the energy dispersion due to finite energy resolution. Anyway, integrating the density over the depth from  $-0.2$  to  $2.0 \mu\text{m}$ , we

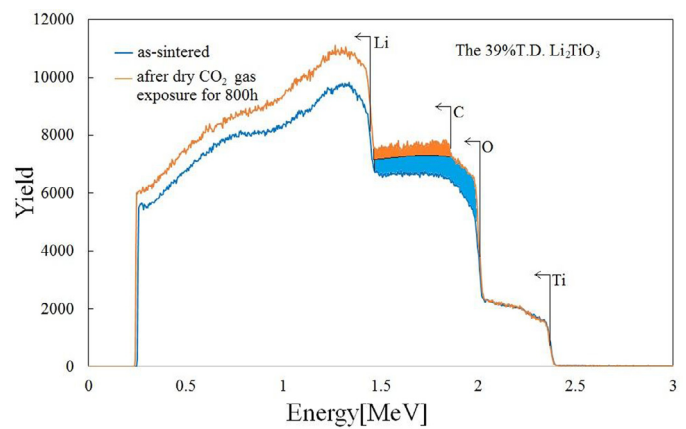


**Fig. 2a.** The NRBS spectra measured with a 2.6-MeV proton beam for non-stoichiometric composition  $\text{Li}_2\text{TiO}_3$  sample (39%T.D.) after exposure to the dry  $\text{CO}_2$  gas for 800 h. The NRBS spectra of the as-sintered  $\text{Li}_2\text{TiO}_3$  sample of the non-stoichiometric composition are also shown for comparison.

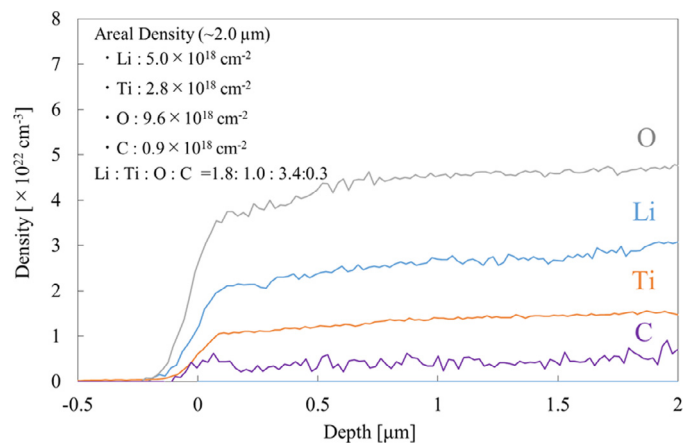


**Fig. 2b.** Depth distribution of Li, C, O and Ti in the non-stoichiometric composition  $\text{Li}_2\text{TiO}_3$  sample (39%T.D.) exposed to the dry  $\text{CO}_2$  gas for 800 h.

obtain the areal densities of Li, C, O and Ti near the surface layers ( $\sim 2.0 \mu\text{m}$ ) as  $N_{\text{Li}} = 5.0 \times 10^{18} \text{ cm}^{-2}$ ,  $N_{\text{C}} = 0.9 \times 10^{18} \text{ cm}^{-2}$ ,  $N_{\text{O}} = 9.6 \times 10^{18} \text{ cm}^{-2}$  and  $N_{\text{Ti}} = 2.8 \times 10^{18} \text{ cm}^{-2}$ , respectively. The composition ratio of Li:Ti:O:C is then 1.8:1.0:3.4:0.3. And the composition ratio of Li:Ti:O before exposure (as-sintered 39%T.D. sample) was 1.8: 1.0: 2.8, which shows O and Li are lost in this sample during sintering in Ar gas atmosphere.

In addition, the dry  $\text{CO}_2$  gas exposure followed by NRBS analysis was also performed on the stoichiometric  $\text{Li}_2\text{TiO}_3$  sample (39% T.D.). Dependence of the C areal density on the exposure time of the dry  $\text{CO}_2$  gas for the non-stoichiometric low-density  $\text{Li}_2\text{TiO}_3$  sample (39%T.D.) and the stoichiometric low-density  $\text{Li}_2\text{TiO}_3$  sample (39%T.D.) is shown in Fig. 3. NRBS analysis was carried out every 200 h. Exposure time of the dry  $\text{CO}_2$  gas was 800 h for the non-stoichiometric sample (39% T.D.) and up to 2,000 h for stoichiometric sample (39% T.D.).

Under the dry  $\text{CO}_2$  gas exposure conditions, the C areal density of the non-stoichiometric sample (39% T.D.) was  $7.5 \times 10^{17} \text{ cm}^{-2}$ ,  $8.6 \times 10^{17} \text{ cm}^{-2}$  and that of the stoichiometric sample was  $1.8 \times 10^{17} \text{ cm}^{-2}$ ,  $4.1 \times 10^{17} \text{ cm}^{-2}$  at an exposure time of 200 h and 400 h, respectively. The non-stoichiometric  $\text{Li}_2\text{TiO}_3$  sample with defects of O and Li deficiencies has 2 to 4 times greater amount of  $\text{CO}_2$  absorbed at the same exposure time compared to the stoichiometric  $\text{Li}_2\text{TiO}_3$  sample. The C areal density of the stoichiometric sample saturates at about 1,200 h, while that of the non-stoichiometric sample (39% T.D.) at about 450 h with almost the same saturation value of  $9 \times 10^{17} \text{ cm}^{-2}$ . Therefore, it is considered that the non-

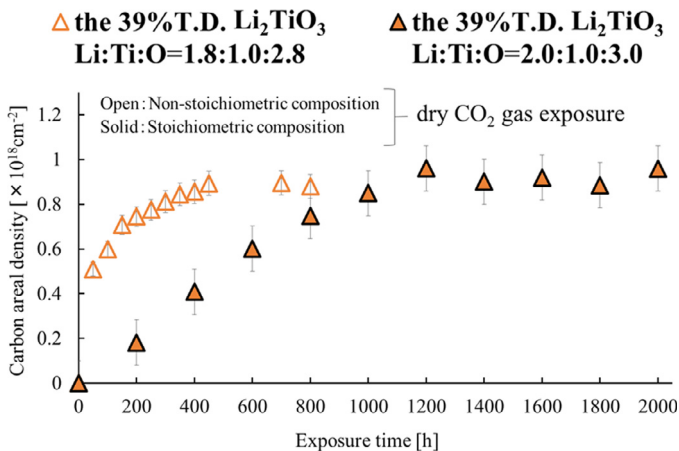


**Fig. 3.** Dependence of C areal density on the exposure time of the dry  $\text{CO}_2$  gas for the non-stoichiometric composition  $\text{Li}_2\text{TiO}_3$  sample (39%T.D.) and the stoichiometric  $\text{Li}_2\text{TiO}_3$  sample (39%T.D.).

stoichiometricity increases  $\text{CO}_2$  absorption rate due to defects of O and Li.

### 3.2. $\text{CO}_2$ absorption characteristics of the $\text{Li}_2\text{TiO}_3$ sample with the optimum density for a blanket material

In order to improve the tritium release characteristics as a blanket material,  $\text{Li}_2\text{TiO}_3$  sample with about 80% T.D. is considered to be good [16–19]. In our previous experiments, it was found that  $\text{CO}_2$  is hardly absorbed by the high-density  $\text{Li}_2\text{TiO}_3$  samples with above 90% T.D. under the atmospheric and the moist air exposures. However,  $\text{Li}_2\text{TiO}_3$  samples with 76%T.D. and 85% T.D. absorbed  $\text{CO}_2$  in the moist air and the atmospheric exposures. Both exposure atmospheres contained  $\text{CO}_2$  with a fraction of 0.035 vol. %.

The high-density  $\text{Li}_2\text{TiO}_3$  sample (91% T.D.) sintered at a temperature above 1,428 K for 40 h absorbed little amount of  $\text{CO}_2$  under the atmospheric exposure for 2,000 h; the crystal structure of the  $\text{Li}_2\text{TiO}_3$  can be seen from the XRD spectrum of this sample after the exposure as shown in Fig. 1. A high-density sample sintered at above 1,428 K was crushed with a crucible and re-sintered at 1,000 K for 10 h. As a result, the 80%T.D.  $\text{Li}_2\text{TiO}_3$  sample was obtained.

The re-sintered 80% T.D. sample was exposed for 1,200 h to the moist air. Fig. 4 shows the dependence of the C areal density in the samples on the exposure time. The re-sintered sample had the C areal density lower than the detection limit in the NRBS measurement for

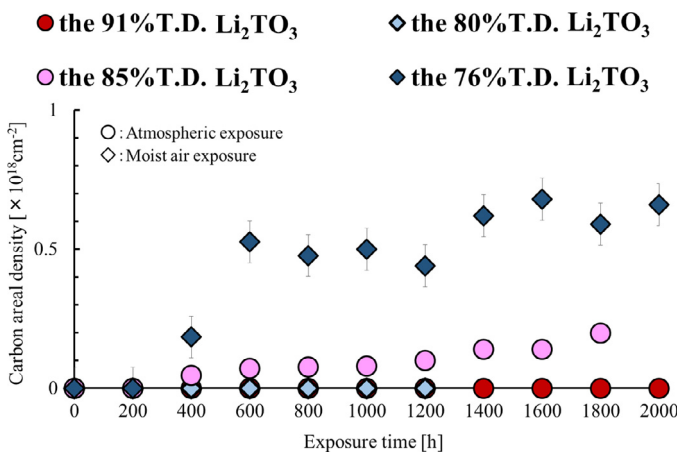


**Fig. 4.** Dependence of C areal density on the exposure time of the atmosphere, and the moist air for the medium- and high-density samples and of the moist air for the sample re-sintered above 1,428 K.

exposure times up to 1,200 h. On the other hand, the C areal density of the 85% T.D. and 76% T.D.  $\text{Li}_2\text{TiO}_3$  samples prepared by sintering at 1,250 K for 8 h and at 1,173 K for 8 h shows  $1.0 \times 10^{17} \text{ cm}^{-2}$  and  $4.4 \times 10^{17} \text{ cm}^{-2}$ , respectively, at the atmospheric and the moist air exposure for 1,200 h.

The 85% T.D.  $\text{Li}_2\text{TiO}_3$  sample sintered at 1,250 K has a higher apparent sample density than the 80% T.D.  $\text{Li}_2\text{TiO}_3$  sample. There is a report by Kleykamp that crystal structure changed from monoclinic to cubic in the  $\text{Li}_2\text{TiO}_3$  sample sintered at above 1,428 K [21]. Taking this into account,  $\text{Li}_2\text{TiO}_3$  was sintered at a temperature above 1,428 K. It is supposed that the crystal structure of  $\text{Li}_2\text{TiO}_3$  turns into cubic one and then turns back to monoclinic one due to the gradual decrease in temperature in the electric furnace. This crystal structure change occurs with rearrangements of the particles and the crystal grains, leaving very few defects such as vacancies and pores, which is supposed to reduce  $\text{CO}_2$  absorption. The XRD peaks in the 80%T.D. sample spectrum have smaller FWHMs compared with others as shown in Fig. 1, which implies the higher crystallinity of the sample.

In summary,  $\text{CO}_2$  absorption is largely influenced by the presence or absence of defects in the  $\text{Li}_2\text{TiO}_3$  sample, and it is suggested that  $\text{CO}_2$  absorption can be greatly suppressed in the sample having very few defects.

### 3.3. Catalytic effect of water vapor on $\text{CO}_2$ absorption in the low-density $\text{Li}_2\text{TiO}_3$ sample

Influence of water vapor on the  $\text{CO}_2$  absorption of the low-density  $\text{Li}_2\text{TiO}_3$  sample has been investigated in a similar manner. The low-density  $\text{Li}_2\text{TiO}_3$  samples (39–41%T.D.) were exposed to the dry air (<5,000 ppm), the atmosphere (20,000 to 30,000 ppm) and the moist air (>34,000 ppm) containing 0.035 vol. %  $\text{CO}_2$  at the room temperature for 2,000 h. ERD analysis was performed every 200 h during exposure to the atmosphere (for 1,800 h), the dry air (800 h) and the moist air (600 h).

The dependence of H areal density on the exposure time of the atmosphere, the dry air and the moist air is shown in Fig. 5. The H areal densities from the sample surface to the depth of 0.5  $\mu\text{m}$  in the 39%T.D.  $\text{Li}_2\text{TiO}_3$  (atmospheric exposure), the 40%T.D. (dry air exposure) and the 41%T.D. (moist air exposure) samples are compared. Although the data scattering is rather large especially for the 39%T.D. sample, it is clear that the value at the moist air exposure is the lowest. In spite of the lower humidity in the dry air and the atmosphere than in the moist air, the H content in the sample with the moist air exposure is the lowest. Therefore, the increase in H content in the sample is not related to the amount of water vapor.

Fig. 6 shows dependence of C areal density on the exposure time to

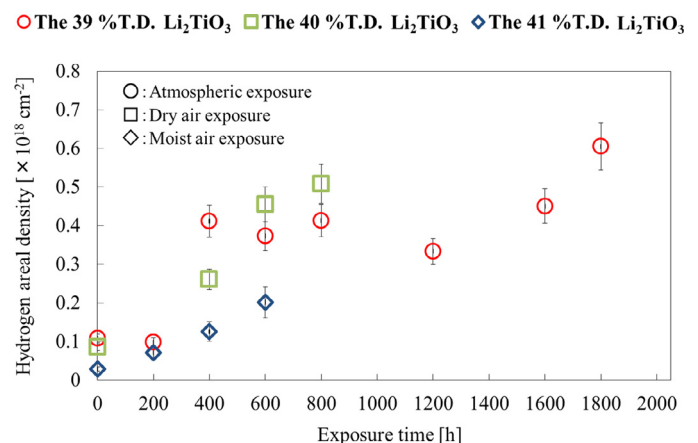


**Fig. 5.** Dependence of H areal density on the exposure time of the dry air, the atmosphere and the moist air for the low-density samples.



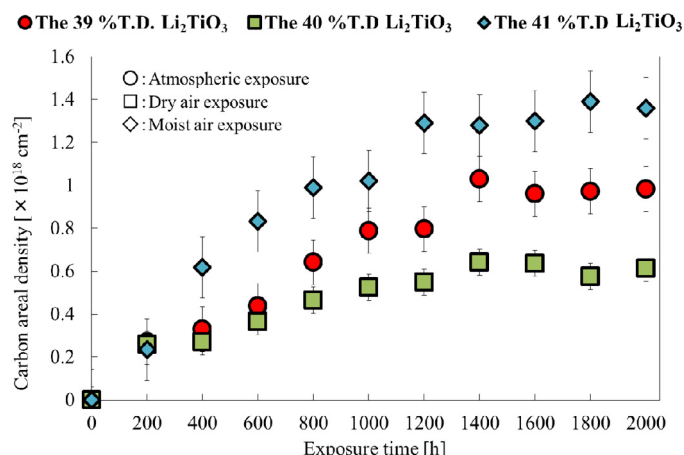


Fig. 6. Dependence of C areal density on the exposure time of the atmosphere, the dry air and the moist air for the low-density samples.

the atmosphere, the dry air and the moist air for the samples. The C areal densities were determined by the NRBS measurement. The C areal densities gradually increased with exposure time until 1,000 h with the saturation values of  $1.3 \times 10^{18} \text{ cm}^{-2}$  (moist air),  $1.0 \times 10^{18} \text{ cm}^{-2}$  (atmosphere) and  $0.6 \times 10^{18} \text{ cm}^{-2}$  (dry air). It is found that the amount of the C areal density under the moist air exposure is the largest.

There is no correlation between the amount of the H areal density and that of the C areal density. This result means that the  $\text{H}_2\text{O}$  absorbed in the sample does not exert any effect on  $\text{CO}_2$  absorption, while the adsorbed  $\text{H}_2\text{O}$  on the sample surface has catalytic effect to promote  $\text{CO}_2$  absorption into the  $\text{Li}_2\text{TiO}_3$  sample.

#### 4. Conclusions

Dry  $\text{CO}_2$  gas exposures of the non-stoichiometric  $\text{Li}_2\text{TiO}_3$  sample with O and Li deficiencies (39%T.D.) and the stoichiometric low-density  $\text{Li}_2\text{TiO}_3$  sample (39%T.D.) have been performed. The XRD analysis shows that in both low-density  $\text{Li}_2\text{TiO}_3$  samples composition of a part of the  $\text{Li}_2\text{TiO}_3$  samples has changed to a mixture of  $\text{Li}_2\text{CO}_3$  and  $\text{TiO}_2$ . The

NRBS analysis of the samples shows that C areal density is increased with exposure time and saturated at about 450 h for the non-stoichiometric sample which is much shorter than 1,200 h for the stoichiometric sample. It is concluded that defects of O and Li deficiencies in the  $\text{Li}_2\text{TiO}_3$  sample promote the  $\text{CO}_2$  absorption.

$\text{CO}_2$  absorption could be greatly suppressed in the sample without defects. We have found a process to prepare a  $\text{Li}_2\text{TiO}_3$  sample that has 80%T.D., the suitable density as the blanket material, and capable of absorbing very little amount of  $\text{CO}_2$  even in high humidity environment.

Next, in order to investigate the influence of water vapor on  $\text{CO}_2$  absorption, exposure experiments have been carried out by changing humidity. ERD measurements have shown that there is no correlation between the H distribution near the  $\text{Li}_2\text{TiO}_3$  sample surface region and the humidity in the atmosphere. On the other hand, NRBS measurements have shown that the amount of the C areal density of the sample exposed to moist air was largest among three exposure conditions. There is no correlation between the amount of H content and the C areal density. It is inferred that adsorbed  $\text{H}_2\text{O}$  on the sample surface provides catalytic action for absorption of  $\text{CO}_2$ .

#### References

- [1] J.P. Kopasz, et al., J. Nucl. Mater. 212–215 (1994) 927–931.
- [2] N. Roux, et al., J. Nucl. Mater. 233–237 (1996) 1431–1435.
- [3] R.F. Mattas, M.C. Billone, J. Nucl. Mater. 233–237 (1996) 72–81.
- [4] A.R. Raffray, et al., J. Nucl. Mater. 307–311 (2001) 21–30.
- [5] A.R. Raffray, J. Nucl. Mater. 307–311 (2002) 21–30.
- [6] H. Kawamura, et al., Nucl. Fusion 43 (2003) 675–680.
- [7] K. Tsuchiya, et al., Nucl. Fusion 47 (2007) 1300–1306.
- [8] T. Hoshino, et al., Fusion Eng. Des. 109–111 (2016) 1114–1118.
- [9] Y. Edao, et al., Fusion Eng. Des. 112 (2016) 480–485.
- [10] Y. Furuyama, J. Nucl. Mater. 442 (2013) S442–S446.
- [11] Y. Furuyama, J. Nucl. Mater. 455 (2014) 527–530.
- [12] Y. Furuyama, Nucl. Mater. and Energy 9 (2016) 227–232.
- [13] S. Nasu, et al., J. Nucl. Mater. 68 (1977) 261–264.
- [14] H. Kudo, et al., J. Inorg. Nucl. Chem. 40 (1978) 363–367.
- [15] S. Ueda, ISIJ Int. 51 (4) (2011) 530–537.
- [16] J.M. Miller, et al., J. Nucl. Mater. 212–215 (1994) 877–880.
- [17] N. Roux, et al., Fusion Eng. Des. 27 (1995) 154–166.
- [18] N. Roux, et al., Fusion Eng. Des. 41 (1998) 31–38.
- [19] J.D. Lulewicz, N. Roux, Fusion Eng. Des. 39–40 (1998) 745–750.
- [20] Y. Furuyama, et al., Nucl. Instrum. Methods Phys. Res. B. 331 (2014) 96–101.
- [21] H. Kleykamp, Fusion Eng. Des. 61–62 (2002) 361–366.